

Direct Observation of Melting in Shock-Compressed Bismuth With Femtosecond X-ray Diffraction

M. G. Gorman,¹ R. Briggs,¹ E. E. McBride,^{1,2} A. Higginbotham,³ B. Arnold,⁴ J. H. Eggert,⁵ D. E. Fratanduono,⁵ E. Galtier,⁴ A. E. Lazicki,⁵ H. J. Lee,⁴ H. P. Liermann,² B. Nagler,⁴ A. Rothkirch,² R. F. Smith,⁵ D. C. Swift,⁵ G. W. Collins,⁵ J. S. Wark,³ and M. I. McMahon¹

¹*SUPA, School of Physics & Astronomy, and Centre for Science at Extreme Conditions, The University of Edinburgh, Edinburgh EH9 3FD, UK*

²*DESY Photon Science, Notkestr. 85, D-22607 Hamburg, Germany*

³*Department of Physics, Clarendon Laboratory, Parks Road, University of Oxford, Oxford OX1 3PU, UK*

⁴*Linac Coherent Light Source, SLAC National Accelerator Laboratory, Menlo Park, California 94025, USA*

⁵*Lawrence Livermore National Laboratory, 6000 East Avenue, Livermore, California 94500, USA*

(Received 15 October 2014; revised manuscript received 26 June 2015; published 28 August 2015)

The melting of bismuth in response to shock compression has been studied using *in situ* femtosecond x-ray diffraction at an x-ray free electron laser. Both solid-solid and solid-liquid phase transitions are documented using changes in discrete diffraction peaks and the emergence of broad, liquid scattering upon release from shock pressures up to 14 GPa. The transformation from the solid state to the liquid is found to occur in less than 3 ns, very much faster than previously believed. These results are the first quantitative measurements of a liquid material obtained on shock release using x-ray diffraction, and provide an upper limit for the time scale of melting of bismuth under shock loading.

DOI: 10.1103/PhysRevLett.115.095701

PACS numbers: 64.70.D-, 62.50.Ef, 81.30.Bx

The study of shock-induced phase transitions, which is vital to understanding material response to rapid pressure changes, dates back to the 1950s when Bancroft *et al.* inferred a structural transition in iron from wave profile measurements [1]. Recent advances in ultrafast probes, such as nanosecond *in situ* x-ray diffraction, have meant that lattice-level studies of such phenomena have become possible [2–4], including the observation of the $\alpha - \epsilon$ transition in iron [5]. These advances give insight into the nature and time scales of the phase transitions, and allow rigorous comparisons to be made with static-compression studies of the same phenomena. However, it has proved a considerable challenge to study the simplest shock-induced phase transition—the melting of a material—using *in situ* diffraction due to the weak signal from liquid samples.

One of the most studied systems in shock-melting experiments is bismuth, due to the accessible pressure-temperature (P - T) range over which melting occurs on both compression and release (see Fig. 1). There have been no direct observations of shock melting in Bi *via* diffraction, but numerous wave profile [6–8] and pyrometry [9] studies have reported melting, or its absence, on both compression and release. The indirect nature of these measurements means that the time scale of melting in Bi remains poorly constrained, with inferred melting times ranging from tens to hundreds of nanoseconds [10,11]. This is longer than the time scale of many laser-driven compression experiments, perhaps explaining the observation of superheated Bi-I, rather than liquid Bi, in the laser-compression study of

Smith *et al.* [7]. These melting time scales are also very much longer than those of a few nanoseconds in which shock-induced solid-solid phase transitions are known to take place in Fe [5] and Bi [12], as determined by diffraction.

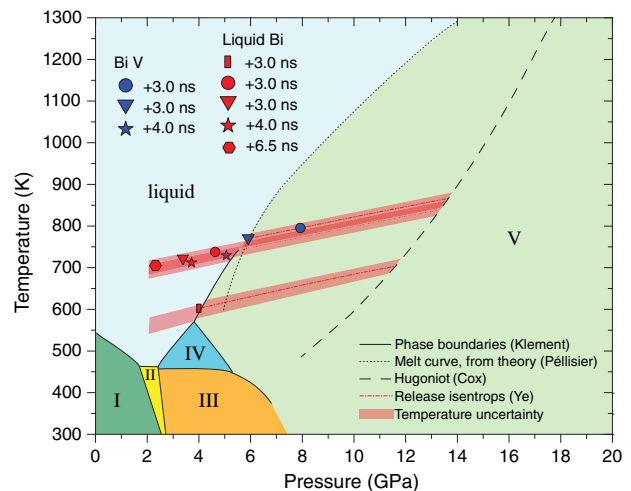


FIG. 1 (color online). The equilibrium phase diagram of Bi to 20 GPa [13,14]. The calculated Principal Hugoniot, the locus of states accessible with a single shock, is shown in the Bi-V phase as a dashed line [15], and the release isentropies from the Hugoniot states, adapted from Ye *et al.* [16], are shown using different dotted-dashed lines. The uncertainty in the position reached on the Hugoniot due to shot-to-shot energy jitter from the drive laser is taken into account and is highlighted by shaded regions around the release isentropies.

Studies of shock melting on compression can be complicated by kinetics, which may result in superheating of the solid phase that can persist for hundreds of nanoseconds or longer [17]. To avoid this we have chosen to study melting in Bi on shock release from the high-pressure Bi-V phase. Such a study also allows a direct comparison with the recent diffraction study of Bi by Hu *et al.*, which reported several solid-solid transitions on release on nanosecond time scales [12]. Here we present femtosecond x-ray diffraction measurements of Bi that provide definitive evidence of liquid diffraction, and which show that on release Bi-V melts within 3 ns at P-T conditions that are in excellent agreement with the equilibrium melt curve [13].

Experiments were performed at the MEC beam line of the Linac Coherent Light Source (LCLS) [18]. A Nd:glass optical laser (527 nm, 20 ns quasi-flat-topped pulses) was used to launch an ablation-driven shock wave through the samples, comprising a 25(3) μm thick polyimide ablator glued to 20(3) μm thick bismuth foil of 99.97% purity (Fig. 2). The epoxy glue layer was approximately 10 μm thick and was well impedance matched with the polyimide ablator. The LCLS provided quasi-monochromatic ($\Delta E/E \sim 0.5\%$) 8.8 keV x-ray pulses of 80 fs duration each containing $\sim 10^{12}$ photons. The x-ray beam was focused to $10 \times 10 \mu\text{m}^2$ and then centered on the $\sim 500 \mu\text{m}$ diameter focal spot of the drive laser, which, in turn, was centered on the target.

2D diffraction images were recorded on CSPAD detectors [19] which were then integrated azimuthally to produce 1D diffraction profiles (Fig. 2) [20]. A VISAR (Velocity Interferometer System for Any Reflector) [23] was used to both record the velocity-time histories of the rear surface of the compressed samples, from which the peak sample pressure was obtained, and to investigate the nonplanarity

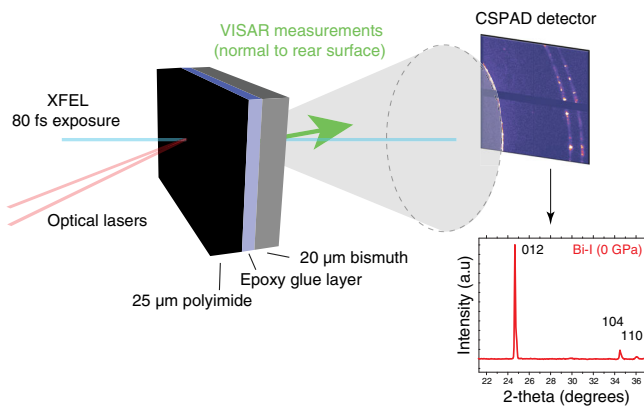


FIG. 2 (color online). Experimental configuration for laser-shock experiments using femtosecond x-ray diffraction at the MEC beam line at LCLS. The VISAR beam is collected perpendicular to the target rear surface (green arrow). 2D diffraction images (top right) are collected on CSPAD detectors in transmission and reflection (not shown) and are then integrated into 1D diffraction profiles (bottom right).

of the drive, which was negligible across the x-rayed region of the target. Additional information on the experimental details and VISAR analysis is given in the Supplemental Material [20].

We studied melting of Bi on release from the high-pressure body-centered cubic (bcc) Bi-V phase, as recently reported by Tan *et al.* [8], which was obtained by shocking the Bi to pressures of between 8 and 14 GPa (see Fig. 1). Breakup of the target rear surface on shock breakout prevented the VISAR from directly determining peak pressures above 10 GPa. Beyond this, the pressure was determined both from a power-law extrapolation of a peak-pressure versus laser-intensity relationship established using the VISAR up to 10 GPa [see Fig. S3(a) in Ref. [20]], and from the density of the Bi-V itself, as determined from the diffraction profiles. The pressures obtained using the two methods were in excellent agreement; see Ref. [20].

Phase transitions within the Bi on release were monitored from changes in the observed diffraction patterns. However, interpretation of these was aided by using the 1D radiation hydrocode package HYADES [24] to model the complex time evolution of the multiple waves within the Bi that arise from the impedance mismatch between the ablator and the sample [25], as illustrated in Fig. 3. This mismatch results in a reshock being generated in the ablator as the initial laser-induced shock is transmitted into the sample. The arrival of this reshock at the ablation front

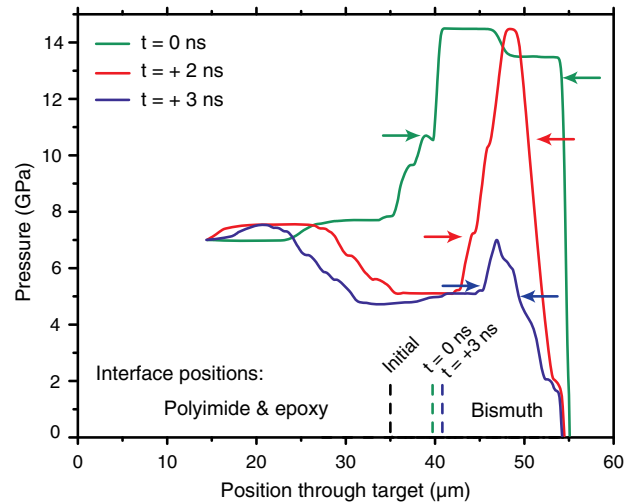


FIG. 3 (color online). Simulated pressure profiles in the Bi targets superimposed on the initial target dimensions. These dimensions change with time and the initial position of the polyimide-epoxy-bismuth interface, and its position at $t = 0$ ns and $t = +3$ ns are shown by the black, green, and blue dashed lines, respectively, at the bottom of the plot. After rear surface breakout, the sample pressure is reduced by both the weak release wave originating at the ablation surface, and by the centered rarefaction wave originating at the rear surface, the propagation directions of which are indicated by arrows.

reduces the drive pressure in the ablator, resulting in the generation of a weak release wave in the sample ($t = 0$ ns profile in Fig. 3, where $t = 0$ is defined as the instance when the VISAR observes the shock wave breaking out at the target rear surface). At later times, this release wave reduces the pressure in the ablator and Bi sample, but maintains the reduced pressure state for the duration of the drive laser pulse ($t = +2$ and $+3$ ns profiles in Fig. 3). In addition to these ablator–Bi wave interactions, the arrival of the initial shock wave at the Bi free surface produces a centered rarefaction wave [26] which propagates backwards in the target, and rapidly releases the sample pressure to zero. Because of the thickness of the ablator and epoxy glue layer, the front surface release wave arrives at the sample after $t = 0$.

These wave interactions result in two distinct P - T states being maintained within the sample for several nanoseconds—a higher-pressure state and a partially released lower-pressure state—both of which are eventually released to zero by the rear surface release wave. Judicious choice of initial drive conditions, and the relative timing of the x-ray exposure, can place the two states on either side of the equilibrium melt curve, enabling the time evolution of melting between them to be studied.

Figures 4(a) and 4(c) (i) show the diffraction pattern collected at $t = -2.0$ ns (i.e., 2 ns before shock breakout) which contains both the (110) Bragg peak from Bi-V at 13.4(3) GPa, along with the (012) peak from the uncompressed Bi-I ahead of the shock front. The marked difference in texture of the Debye-Scherrer (D-S) rings suggests that the grain size of Bi-V is significantly smaller than that of the uncompressed Bi-I: from the smoothness of the Bi-V rings, we estimate its grain size as submicron. This is in marked contrast to the behavior observed in static compression experiments, where significant grain growth is observed in the high-pressure phases of Bi [27].

At $t = +3.0$ ns [Figs. 4(b) and 4(c) (ii)], the diffraction pattern is dominated by a broad diffuse ring of scattering that unequivocally indicates the presence of liquid Bi. A weak Bi-V (110) peak is also observed, originating from the remaining higher-pressure region of the sample, as well as a weak Bi-I (012) peak which most likely originates from that sample material that has been fully released to zero pressure by the rarefaction wave. The smoothness of the D-S rings from the fully released Bi-I is very different to the highly textured rings of the starting material [compare Figs. 4(a) and 4(b)], suggesting that the rapid ($\sim 10^9$ GPa/sec) release to ambient pressure results in the creation of very small (we again estimate submicron) crystallites.

The pressures in the solid and liquid regions of the sample at $t = +3.0$ ns are different as a result of the wave interactions (Fig. 3), and each can be determined experimentally by comparing the solid and liquid diffraction

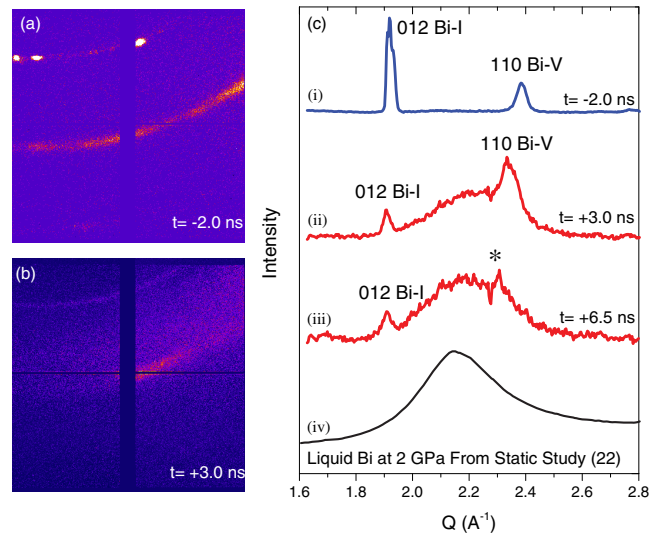


FIG. 4 (color online). Raw and integrated diffraction profiles collected at different times relative to rear surface breakout ($t = 0$). At $t = -2.0$ ns [(a) and (c)(i)] both the high-pressure Bi-V (110) peak and the Bi-I (012) peak from the as-yet uncompressed sample are observed. At $t = +3.0$ ns [(b) and (c)(ii)], the profiles are dominated by a broad liquid diffraction peak from the melted region of the sample. The liquid diffraction signal is still observed at $t = +6.5$ ns [profile (c)(iii)] at which time the Bi-V (110) peak has disappeared. The origin of the peak marked with an asterisk is discussed in Ref. [28]. A diffraction profile from liquid Bi obtained in a diamond anvil cell study at 2 GPa and 500 K [29,30] is shown in profile (c)(iv) for comparison.

patterns with those obtained in previous static-compression studies of the same phases. The Bi-V (110) peak at $t = +3.0$ ns is at $Q = 2.35 \text{ \AA}^{-1}$, which corresponds to a pressure of 7.9(2) GPa, as determined from a high-temperature Mie-Grüneisen-Debye equation of state (EOS), and the 300 K isothermal EOS [31]. The liquid diffraction peak is at $Q \sim 2.22 \text{ \AA}^{-1}$, which, comparing to previous diffraction data from liquid-Bi (see Fig. S4 [20]), corresponds to a lower pressure of 4.7(8) GPa. These pressures are in good agreement with the HYADES simulations, which at $t = +3.0$ ns predict a $\sim 5 \text{ \mu m}$ thickness of the sample is at 6–7 GPa while a $\sim 6 \text{ \mu m}$ thickness has partially released to 4.5 GPa, and is therefore in the liquid phase (Fig. 3).

At $t = +6.5$ ns, the liquid diffraction signal persists [Fig. 4(c) (iii)], but no diffraction from Bi-V is observed, indicating that all of this phase has either melted or been released to ambient pressure [28]. For comparison with the data obtained in this study, Fig. 4(c) (iv) shows a diffraction profile from liquid-Bi at 2 GPa and 500 K obtained during the synchrotron study of Bi-IV by Chaimayo *et al.* [29,30]. The similarity of the two profiles confirms that what we observe here is indeed liquid-Bi, formed on nanosecond time scales on shock release from Bi-V. Other mechanisms which could generate a similar diffraction pattern, such as

strain gradients or particle size broadening in Bi-V, can be discounted due to the unphysical lattice parameters or pressure gradients required.

The key finding of this study is that liquid scattering is observed at $t = +3.0$ ns, but not at shock breakout ($t = 0$ ns). Within 3 ns, therefore, sufficient sample has melted in order to give a measurable diffraction signal, thus placing an upper limit on the timescale of melting. We observed release melting in 11 targets, four of which constrained the melting time to < 3 ns, and one to < 4 ns, with the others providing no better constraints. This time scale is very much shorter than previous estimates for shock melting in Bi, which ranged from tens to hundreds of nanoseconds [10,11]. However, these estimates were obtained from the modeling of Bi wave profiles, which can be very complex [32], and which also require assumptions as to which profile features are indicative of melting. This is nontrivial, and even in the most recent study [8] it was not possible to say whether the “knees” seen in the release wave profiles definitely resulted from melting of Bi-V, but only that this was a possibility.

However, by directly determining all of the phases present in our samples using 80 fs x-ray exposures, our data show unequivocally that Bi melts within 3 ns on release from Bi-V. We note that a recent diffraction study of the solid-solid phase transitions in Bi on shock release from lower pressures [12], using 100 ps x-ray exposures, found three successive phase transitions—Bi-V \rightarrow Bi-III \rightarrow Bi-II \rightarrow Bi-I—to occur within 30 ns, with individual transition times similar to the melting time reported here. Ultrafast x-ray diffraction is thus an excellent way of unambiguously determining both the nature and time scale of shock-induced phase transitions on the nanosecond time scales of laser compression experiments. The 3 ns melting time scale reported here is an upper limit, however, and further studies with higher time resolution may find that melting occurs faster still. We note that nonequilibrium nonthermal melting in thin Bi films has been shown to occur within only 190 fs [33].

Interpreting the results of previous melting studies of Bi under dynamic compression—without definitive confirmation of the sample state—has often relied on comparisons to the equilibrium phase diagram. However, it remains unclear whether the phases and transitions observed are the same as those found using static techniques. Our diffraction data allow such a comparison.

A shock wave is an extremely efficient way of internally heating a material on nanosecond time scales, producing heating rates of $\sim 10^{12}$ K/s for a strong shock [34]. This can result in specific shock-melting phenomena such as superheating (undercooling), where melting occurs at temperatures above (below) the equilibrium melt curve. Such phenomena have been the subject of numerous computational and experimental studies, with the computational

study of Luo *et al.* [34] reporting that Bi should be particularly susceptible to such effects due to its large nucleation energy barrier.

Figure 1 shows the P - T states of bismuth accessed in this study on shock release, plotted on the equilibrium phase diagram. The states all lie on release isentropes from the Principal Hugoniot [16] and in each sample where melting was observed the pressures of the solid and liquid phases were determined experimentally from the diffraction patterns—see Ref. [20] for full details. The P - T conditions at which solid and liquid phases are found are in excellent agreement with the equilibrium melt curve (Fig. 1): within the uncertainties we see no evidence of any superheating of Bi-V in the liquid region [35].

The absence of superheating, and the fast melting time for Bi reported here, may result from the fact that we are studying release melting of polycrystalline Bi-V created by shock compression. Polycrystalline samples will contribute to the suppression of superheating as they possess more defects than single crystals, thus providing more nucleation sites for the liquid phase [36]. Our diffraction data show that the Bi-V grain size is much smaller than that of the starting material, further increasing the number of nucleation sites. Finally, the shock wave that created the Bi-V is itself a proficient generator of dislocations in the sample, which will further increase the number of nucleation sites, thereby suppressing superheating and aiding homogeneous melting.

The agreement between the melting conditions reported here and the equilibrium phase diagram means that dynamic compression techniques, coupled with x-ray diffraction, have great promise for extending equilibrium melt curves to P - T conditions currently inaccessible to static compression methods. Such techniques have already been used successfully to study solids in the terapascal regime [37], and the ability of diffraction to discriminate solids from liquids will enable melting studies to be extended to similar pressures. Of particular importance will be the ability to distinguish melting [38] from solid-solid phase transitions that may occur close to the melt curve, as has been suggested in iron [39], carbon [40,41], and magnesium oxide [42], and to identify melting in materials where the absence of any accompanying density change may prevent its identification *via* wave profile analysis.

M. I. M. and J. S. W. would like to acknowledge support from EPSRC under Grant No. EP/J017256/1. The work by J. H. E., D. E. F., A. E. L., R. F. S., D. C. S., and G. W. C. was performed under the auspices of the U.S. Department of Energy by Lawrence Livermore National Laboratory under Contract DE-AC52-07NA27344. We thank D. Milathianaki and C. Bolme for their help during the experiment with target chamber setup and calibration of the VISAR system. We also thank S. McWilliams for useful discussions and contributions in preparation of the

manuscript. Use of the Linac Coherent Light Source (LCLS), SLAC National Accelerator Laboratory, is supported by the U.S. Department of Energy, Office of Science, Office of Basic Energy Sciences under Contract No. DE-AC02-76SF00515. The MEC instrument is supported by the U.S. Department of Energy, Office of Science, Office of Fusion Energy Sciences under Contract No. SF00515.

-
- [1] D. Bancroft, E. L. Peterson, and S. Minshall, *J. Appl. Phys.* **27**, 291 (1956).
- [2] Q. Johnson and A. Mitchell, *Phys. Rev. Lett.* **29**, 1369 (1972).
- [3] T. d'Almeida and Y. M. Gupta, *Phys. Rev. Lett.* **85**, 330 (2000).
- [4] J. R. Rygg, J. H. Eggert, A. E. Lazicki, F. Coppari, J. A. Hawreliak, D. G. Hicks, R. F. Smith, C. M. Sorce, T. M. Uphaus, B. Yaakobi, and G. W. Collins, *Rev. Sci. Instrum.* **83**, 113904 (2012).
- [5] D. H. Kalantar, J. F. Belak, G. W. Collins, J. D. Colvin, H. M. Davies, J. H. Eggert, T. C. Germann, J. Hawreliak, B. L. Holian, K. Kadau, P. S. Lomdahl, H. E. Lorenzana, M. A. Meyers, K. Rosolankova, M. S. Schneider, J. Sheppard, J. S. Stölkén, and J. S. Wark, *Phys. Rev. Lett.* **95**, 075502 (2005).
- [6] J. R. Asay, *J. Appl. Phys.* **45**, 4441 (1974).
- [7] R. F. Smith, J. H. Eggert, M. D. Saculla, A. F. Jankowski, M. Bastea, D. G. Hicks, and G. W. Collins, *Phys. Rev. Lett.* **101**, 065701 (2008).
- [8] Y. Tan, Y. Yu, C. Dai, K. Jin, Q. Wang, J. Hu, and H. Tan, *J. Appl. Phys.* **113**, 093509 (2013).
- [9] D. Partouche-Sebban and J. L. Pelissier, *Shock Waves* **13**, 69 (2003).
- [10] D. B. Hayes, *J. Appl. Phys.* **46**, 3438 (1975).
- [11] M. Bastea, S. Bastea, J. Emig, P. Springer, and D. Reisman, *Phys. Rev. B* **71**, 180101 (2005).
- [12] J. Hu, K. Ichiyangi, T. Doki, A. Goto, T. Eda, K. Norimatsu, S. Harada, D. Horiuchi, Y. Kabasawa, S. Hayashi, S.-i. Uozumi, N. Kawai, S. Nozawa, T. Sato, S.-i. Adachi, and K. G. Nakamura, *Appl. Phys. Lett.* **103**, 161904 (2013).
- [13] W. Klement, A. Jayaraman, and G. Kennedy, *Phys. Rev.* **131**, 632 (1963).
- [14] J. L. Pelissier and D. Partouche-Sebban, *Physica B (Amsterdam)* **364**, 14 (2005).
- [15] G. A. Cox, *AIP Conf. Proc.* **955**, 151 (2007).
- [16] T. Ye, Y. Yu-Ying, D. Cheng-Da, Y. Ji-Dong, W. Qing-Song, and T. Hua, *Acta Phys. Sin.* **62**, 036401 (2013).
- [17] D. A. Boness and J. M. Brown, *Phys. Rev. Lett.* **71**, 2931 (1993).
- [18] B. Nagler *et al.*, *J. Synchrotron Radiat.* **22**, 520 (2015).
- [19] P. Hart, S. Boutet, G. Carini, A. Dragone, B. Duda, D. Freytag, G. Haller, R. Herbst, S. Herrmann, C. Kenney, J. Morse, M. Nordby, J. Pines, N. van Bakel, M. Weaver, and G. Williams, in *2012 IEEE Nuclear Science Symposium and Medical Imaging Conference (2012 NSS/MIC)* (IEEE, Bellingham, WA, 2012), p. 538.
- [20] See Supplemental Material <http://link.aps.org/supplemental/10.1103/PhysRevLett.115.095701> for additional information on the experiment, pressure determination, and simulations, which includes Refs. [21–22].
- [21] K. T. Lorenz, M. J. Edwards, S. M. Pollaine, R. F. Smith, and B. A. Remington, *High Energy Density Phys.* **2**, 113 (2006).
- [22] K. Yaoita, K. Tsuji, Y. Katayama, and M. Imai, J. Chen, T. Kikegawa, O. Shimomura, *J. Non-Cryst. Solids* **150**, 25 (1992).
- [23] P. M. Celliers, D. K. Bradley, G. W. Collins, D. G. Hicks, T. R. Boehly, and W. J. Armstrong, *Rev. Sci. Instrum.* **75**, 4916 (2004).
- [24] J. T. Larsen and S. M. Lane, *J. Quant. Spectrosc. Radiat. Transfer* **51**, 179 (1994).
- [25] D. C. Swift and R. G. Kraus, *Phys. Rev. E* **77**, 066402 (2008).
- [26] J. W. Forbes, *Shockwave Compression of Condensed Matter* (Springer, New York, 2012), p. 38.
- [27] M. I. McMahon, O. Degtyareva, and R. J. Nelmes, *Phys. Rev. Lett.* **85**, 4896 (2000).
- [28] The small peak marked with an asterisk in Fig. 4(c) (iii) is an edge effect from the tiled detector, and is not a diffraction peak—it is anomalously sharp, and its position is incorrect for Bi-V.
- [29] W. Chaimayo, L. F. Lundegaard, I. Loa, G. W. Stinton, A. R. Lennie, and M. I. McMahon, *High Press. Res.* **32**, 442 (2012).
- [30] These unpublished liquid data were collected at pressures between 1.3 and 3.1 GPa at 500 K during experiments to grow a single crystal of Bi-IV from the melt [29].
- [31] Y. Akahama, H. Kawamura, and A. K. Singh, *J. Appl. Phys.* **92**, 5892 (2002).
- [32] Z. Rosenberg, *J. Appl. Phys.* **56**, 3328 (1984).
- [33] G. Sciaïni, M. Harb, S. G. Kruglik, T. Payer, C. T. Hebeisen, F.-J. Meyer zu Heringdorf, M. Yamaguchi, M. Horn-von Hoegen, R. Ernstorfer, and R. J. Dwayne Miller, *Nature (London)* **458**, 56 (2009).
- [34] S. N. Luo, T. J. Ahrens, T. Cagin, A. Strachan, W. A. Goddard, and D. C. Swift, *Phys. Rev. B* **68**, 134206 (2003).
- [35] One solid point (at 5 GPa and 720 K) lies just within the liquid region of the equilibrium phase diagram. However, a shift of only 25 K in the release isentrope would place it back within the solid region, well within the systematic errors that arise from fluctuations of the laser energy shot-to-shot (approximately 1 J).
- [36] G. I. Kanel, S. V. Razorenov, K. Baumung, and J. Singer, *J. Appl. Phys.* **90**, 136 (2001).
- [37] F. Coppari, R. F. Smith, J. H. Eggert, J. Wang, J. R. Rygg, A. Lazicki, J. A. Hawreliak, G. W. Collins, and T. S. Duffy, *Nat. Geosci.* **6**, 926 (2013).
- [38] L. B. Fletcher *et al.*, *Nat. Photonics* **9**, 274 (2015).
- [39] J. H. Nguyen and N. C. Holmes, *Nature (London)* **427**, 339 (2004).
- [40] J. H. Eggert, D. G. Hicks, P. M. Celliers, D. K. Bradley, R. S. McWilliams, R. Jeanloz, J. E. Miller, T. R. Boehly, and G. W. Collins, *Nat. Phys.* **6**, 40 (2010).
- [41] M. D. Knudson, M. P. Desjarlais, and D. H. Dolan, *Science* **322**, 1822 (2008).
- [42] R. S. McWilliams, D. K. Spaulding, J. H. Eggert, P. M. Celliers, D. G. Hicks, R. F. Smith, G. W. Collins, and R. Jeanloz, *Science* **338**, 1330 (2012).